銀などに関して，タンパク質と同等のサブナノサイズ領域（10 nm 以下）の素材（サブナノ素材）の開発・実用化も進んでいる。しかし現状では，地球規模でナノマテリアルやサブナノ素材の安全性に警鐘が鳴らされ，OECD を含め，欧米では規制が進んでいるものの，わが国を鑑みると，薬事法・薬局方（医薬品・化粧品・医薬部外品など）をはじめとする各種法律を見ても，ナノマテリアルやサブナノ素材に言及した規制はない。さらに，これら各種法律においては，ナノマテリアルやサブナノ素材を構成する化学物質の構造式（物質名）のみで規制されているため，従前のサブミクロンサイズ（100 nm）以上の素材で安全性が確認されたものや，経験的に安全と考えられるものであれば，ナノ化・サブナノ化されたものでも自由に利用できてしまうことになる。すなわち，①ナノ化・サブナノ化によって，安全性を運命づける『動態特性や効能・効果』が，同一素材であっても，従前のサブミクロンサイズ以上の素材や分子状素材と大きく変動し得ること，②物性などによっても，ナノマテリアルやサブナノ素材に特有の性能が変動し得ること，が理解されつつあるにもかかわらず，品質管理・保障の規制・ガイドライン策定には程遠いのが現状である。したがって，今後は，物性・品質と，動態情報や安全性情報の連関解析を定量的に実施する必要があると考えられる。このように，Nano-Safety Science の視点から，ナノマテリアルの安全性情報を収集したうえで，Nano-Safety Design の視点から，安全性の高いものは実用化を推進し，安全性の低いものは表面性状制御をはじめとした適切な方策を講じて安全性を高めていくことで，ヒト健康の確保と同時に，われわれがナノテクノロジーの恩恵を享受しつつナノ産業界の発展も達成できるものと考えている。今後，ナノ開発研究とナノ安全科学研究が強固に連携し，両輪となってともに歩むことで，Sustainable Nanotechnology（いわゆる，持続可能なナノテクノロジー）に資する，地球・環境・ヒトに優しい（安全な）ナノマテリアルの創製，ひいてはナノ医薬品の開発が飛躍的に進歩することを楽しみに，筆者らも一緒にチャレンジしたい。

**【引用・参考文献】**


1) K. Ajima, et al.：*Mol. Pharm.*, **2**, 475 (2005).
2) Y. Tabata, et al.：*Jpn. J. Cancer Res.*, **88**, 1108 (1997).
3) C. A. Poland, et al.：*Nat. Nanotechnol.*, **3**, 423 (2008).
4) G. Oberdörster, et al.：*J. Nanosci. Nanotechnol.*, **9**, 4996 (2009).
5) H. Nabeshi, et al.：*Part. Fibre Toxicol.*, **8**, 1 (2011).
6) T. Yoshida, et al.：*Nanoscale Res. Lett.*, **6**, 195 (2011).
7) K. Yamashita, et al.：*Inflammation*, **33**, 276 (2010).
8) H. Nabeshi, et al.：*Biomaterials*, **32**, 2713 (2011).
9) K. Yamashita, et al.：*Nat. Nanotechnol.*, **6**, 321 (2011).


〈東阪　和馬／堤　康央〉

Tetrahedron Letters 54 (2013) 3510–3513

Contents lists available at SciVerse ScienceDirect

Tetrahedron Letters

journal homepage: www.elsevier.com/locate/tetlet

# Synthesis and characterization of new acetalized [60]fullerenes

Ken Kokubo *, Hiroyuki Masuda, Naohiko Ikuma, Tsubasa Mikie, Takumi Oshima

*Division of Applied Chemistry, Graduate School of Engineering, Suita, Osaka 565-0871, Japan*

ARTICLE INFO

*Article history:*
Received 22 March 2013
Revised 18 April 2013
Accepted 22 April 2013
Available online 29 April 2013

*Keywords:*
Fullerene
Acetalization
Cyclic acetal
n-Type material
Organic thin-film solar cell

ABSTRACT

Acetalized [60]fullerenes were synthesized from cyclohexanone-fused [60]fullerene, which was facilely prepared by Diels–Alder reaction of $C_{60}$ with silylether diene, on treatment of various aliphatic alcohols under $TiCl_4$ catalyst. The spiro-cyclic acetalized [60]fullerenes having five, six, and seven-membered rings were also synthesized by using the corresponding diols under the same condition. The slightly raised reduction potentials $E^{red}$ (~0.04 V) relative to those of PCBM were observed by cyclic voltammetry measurement, depending on the identity of alkyl group/chain. The noncyclic acetalized [60]fullerenes showed lower thermal stability up to 200 °C, while the cyclic ones exhibited the drastically improved thermal stability up to 350 °C under nitrogen atmosphere. The acid-catalyzed hydrolysis easily removed the acetal moiety quantitatively, resulting in a considerable change of solvent solubility of the fullerene.



Chemically functionalized fullerenes have recently attracted much attention as n-type semiconductor materials owing to their slightly raised LUMO energy level relative to the pristine $C_{60}$ and the improved solubility required both for wet processing to fabricate thin film and for co-mixing with p-type materials represented by P3HT.[1] The most widely used n-type fullerene derivative is [6,6]-phenyl-$C_{61}$-butyric acid methyl ester, PCBM, and many researches have been devoted to properly raise the LUMO level by minor[2] or major (e.g., SIMEF and ICBA)[3] modifications to increase the open-circuit voltage and the resulting power conversion efficiency on organic thin-film solar cells.

To develop versatile synthetic methods for a series of requisite derivatives, a key precursor fullerene is desired to fulfill some intrinsic properties such as facile accessibility with high mono-adduct selectivity, easy purification, further modifiability, and sufficient stability. One of the most promising candidates to be applicable is cyclohexanone-fused fullerene **1**[4] which has a less congested carbonyl group capable of being converted into some functional groups, such as alcohol/ester[4,5] and imine/amine.[6] However, the introduction of other possible groups to **1** including acetal group has not been reported yet.

Acetal group can be introduced by a simple nucleophilic attack of alcohols to a carbonyl group of **1** and thus various alcohols can be employed to tune its electronic properties desired as n-type materials. Moreover, the acetal group can be deprotected by simple hydrolysis with an acid catalyst in order to change the solvent solubility. Such control of fullerene solubility could be very useful in multi-layered wet fabrication process[7] as well as in nanolithography.[8] However, only a few examples of acetalized fullerene have been hitherto synthesized incidentally.[9]

Herein we report a facile synthesis of new acetalized [60]fullerenes **2** and **3** by $TiCl_4$-mediated reaction of cyclohexanone-fused fullerene **1** with several alcohols. Their electronic properties as well as the thermal stability seem to make them as a new candidate for n-type materials.

The Diels–Alder reaction of $C_{60}$ with a slight excess of 2-trimethylsilyloxy-1,3-butadiene (1.1 equiv) was carried out in toluene at reflux temperature for 24 h by a previously reported method[4] (Scheme 1). The resulting [2+4] adduct was readily

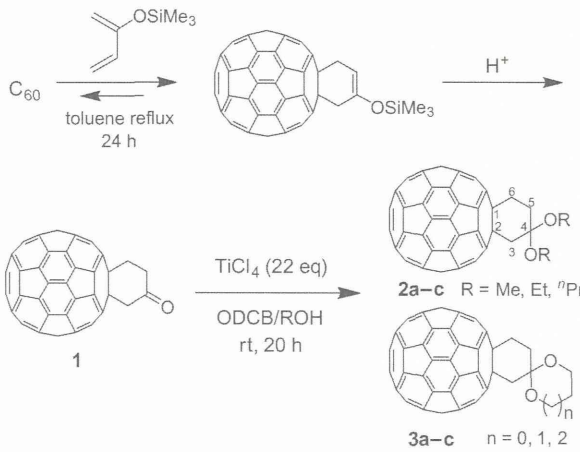


**Scheme 1.** Synthesis of acetalized fullerenes **2** and **3** by the reaction of cyclohexanone-fused **1** with various alcohols and diols.

* Corresponding author. Tel.: +81 6 6879 4592; fax: +81 6 6879 4593.
*E-mail address:* kokubo@chem.eng.osaka-u.ac.jp (K. Kokubo).

0040-4039/$ - see front matter © 2013 Elsevier Ltd. All rights reserved.
http://dx.doi.org/10.1016/j.tetlet.2013.04.093

**Table 1**
$TiCl_4$-mediated acetalization of cyclohexanone-fused 1 with various alcohols[a]

| 2/3 | Alcohol | Temp. (°C) | Conv[b] (%) | Yield[b,c] (%) | Isolated yield (%) |
|---|---|---|---|---|---|
| **2a** | MeOH | rt | 67 | >99 | 61 |
| **2b** | EtOH | rt | 40 | >99 | 36 |
| **2c** | 1-PrOH | rt | 28 | >99 | 27 |
| — | 2-PrOH | 50 | tr[d] | — | — |
| **3a**[e] | $HO(CH_2)_2OH$ | rt | 80 | >99 | 73 |
| **3b**[e] | $HO(CH_2)_3OH$ | rt | 93 | >99 | 65 |
| **3c**[e] | $HO(CH_2)_4OH$ | rt | 52 | >99 | 35 |

[a] The reaction of **1** (100 mg) with alcohol (6 mL) was carried out in the presence of $TiCl_4$ (300 μL, 22 equiv) in ODCB (20 mL) for 20 h.
[b] Determined by HPLC.
[c] Based on $C_{60}$ consumed.
[d] Trace amount.
[e] In ODCB/THF/alcohol (10/10/2 in mL).

decomposed on silica gel column chromatography to afford cyclohexanone-fused fullerene **1** in good yield (65%). In general, Diels–Alder [2+4] adduct of $C_{60}$ is likely to undergo retro-reaction. However, the present Diels–Alder reaction is designed to avoid the retro-reaction by the following facile desilylation, giving the thermally stable monoadduct **1**. The bisadducts were also detected by HPLC using a Buckyprep column (~15%) as a mixture of the isomers.

The reactions of **1** with various alcohols in the presence of $TiCl_4$ (ca. 20 equiv) were carried out in *o*-dichlorobenzene (ODCB)/alcohol (20/6 by v/v) at room temperature for 20 h by modification of the reported method[10] (Table 1). Tracing with HPLC, the reaction was quenched by the addition of triethylamine (500 μL) and acetals **2/3** were isolated by silica gel column chromatography ($CS_2$/ethyl acetate = 9/1 for **2a**; $CS_2$/diethyl ether = 94/6 for **3b**; toluene for others). The conversion for **2a–c** decreased in the order of alcohol alkyl groups Me **2a** <Et **2b** <$^n$Pr **2c** due to the increased steric bulk. The secondary alcohol 2-PrOH was hardly reacted due to the unendurable steric hindrance. The diols $HOCH_2CH_2(CH_2)_nOH$ ($n$ = 0–2) were reacted with **1** to give a good to fair amount of the spiro-cyclic acetals **3a–c** by using a mixed-solvent of ODCB/THF (10/10 by v/v) in order to improve the mixability of diols to ODCB. Because acetalization is a reversible reaction, all alcohols and solvents used were dried and distilled before use. Nevertheless, a stoichiometric amount of $TiCl_4$ was needed for the satisfied conversion due to its deactivation by the stoichiometrically formed water. Some unidentified byproducts, probably the hemiacetals and the noncyclic acetal, were also formed when we used ethylene glycol as purchased.

The structures of **2/3** were determined by $^1$H and $^{13}$C NMR analysis and MALDI-TOF-MS spectroscopy.[11] The $^1$H NMR spectrum of **2a** (in $CS_2/CDCl_3$) showed two sets of ddd (observed as multiplet) protons at 3.05 and 3.50 ppm (both 2H), which were assigned to the cyclohexyl methylene protons on C5 and C6 carbons, respectively. Other two singlet protons at 3.53 (6H) and 3.74 (2H) ppm were assigned to methoxy and isolated methylene (C3) protons. Such a large down-field shift for C6- and C3-methylene protons is clearly due to the strong electron-withdrawing effect of the fullerenyl moiety as well as the acetal moiety. The sharp peak for these singlet protons indicates that the cyclohexane ring is somewhat flexible to flip in the time scale of NMR at room temperature. The $^{13}$C NMR of **2a** showed 7 aliphatic $sp^3$ signals including an acetalic carbon (101.96 ppm) and 28 signals in $sp^2$ fullerene region indicating $C_S$ symmetry of the fullerenyl moiety. The high resolution MALDI-TOF-MS exhibited the molecular ion peak at 836 $m/z$ in negative mode. The $^1$H NMR spectra of **2b** and **2c** showed similar characteristics to those of **2a**, while the α-methylene protons in each alkoxy group showed a slightly different chemical shift due to the difference in axial/equatorial positions. The cyclic acetals **3a–c** also showed essentially the same $^{13}$C signal patterns to **2a** with an acetalic carbon peak at around 100 ppm and 28 $sp^2$ fullerenyl signals.

To elucidate the electronic property of acetalized fullerenes, the reduction potentials of **1**, **2c**, and **3b**, and PCBM were measured by cyclic voltammetry using Ag/AgCl reference electrode and Pt as both working and counter electrode in ODCB (Fig. 1). All cyclic voltammograms showed clear three pairs of reversible peaks in reduction region. The first reduction potential $E_1$ (V vs $Fc/Fc^+$) of ketone **1** was the same as that of PCBM (−1.17) (Table 2). However, those of compounds **2** and **3** (−1.21) were slightly shifted to negative potential up to 0.03–0.04 V due to the electron-donating ability of the alkoxy substituent as compared with those of **1** and PCBM. The slightly raised LUMO level has been reported to be effective to increase the open-circuit voltage $V_{OC}$, which is a key factor on power conversion efficiency (PCE) in an organic thin layer solar cell.[13] The slightly higher LUMO level of acetals **2/3** would be expected to exhibit the larger $V_{OC}$ than that of PCBM in the combination of P3HT.

Considering that acetal C–O bond seems to be easily degraded as compared to the simple ether bond, the thermal stabilities of **2** and **3** were measured by thermogravimetric analysis under nitrogen atmosphere (Fig. 2). The noncyclic acetal **2a** showed a rather lower decomposition temperature at 200 °C, while cyclic acetals **3** exhibited the excellent stability up to 350 °C for **3a**, 320 °C for **3b**, and 270 °C for **3c**. The gradual weight loss for **3** from 150 °C as compared with that of **2a** is probably due to the residual solvent or diol, because we confirmed no change of the sample after heating up to 280 °C under nitrogen by HPLC analysis. The weight loss of **3** up to this temperature is less than 2 wt % and does not correspond to the wt % of diol moiety (5.3–8.4 wt % for **3a–c**). In

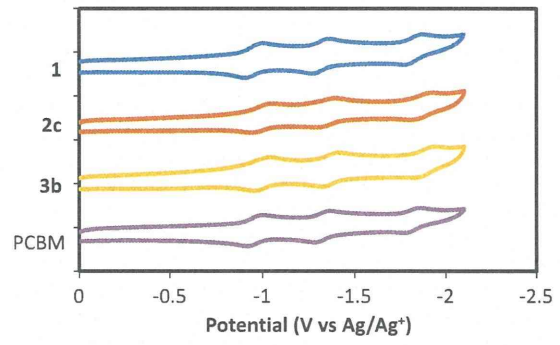


**Figure 1.** Cyclic voltammograms of fullerene derivatives **1**, **2c**, **3b** and PCBM in ODCB.

**Table 2**
Reduction potentials of fullerenes **1–3** and PCBM in ODCB

| | $E^{red}$ V versus $Fc/Fc^{+a}$ | | | LUMO[b] (eV) |
|---|---|---|---|---|
| | $E_1$ | $E_2$ | $E_3$ | |
| $C_{60}$ | −1.09 | −1.47 | −1.92 | −3.71 |
| **1** | −1.17 | −1.53 | −2.04 | −3.63 |
| **2a** | −1.20 | −1.57 | −2.11 | −3.60 |
| **2b** | −1.21 | −1.57 | −2.11 | −3.59 |
| **2c** | −1.21 | −1.56 | −2.11 | −3.59 |
| **3b** | −1.21 | −1.58 | −2.12 | −3.59 |
| PCBM | −1.17 | −1.54 | −2.03 | −3.63 |

[a] Reduction potentials $E_{red}$ = 0.5 ($E_p^{ox} + E_p^{red}$) were measured versus Ag/AgCl reference electrode and standardized to $Fc/Fc^+$ couple $E_{Fc/Fc^+}$ = +0.215 V versus $Ag/Ag^+$ (ODCB)] in 0.1 mM ODCB with 0.1 M $^n Bu_4PF_6$ as supporting electrolyte. Scan rate was 100 mV/s.
[b] Calculated from $E_1$ using LUMO level = $-e$ ($E_1^{red}$ + 4.8).[12]

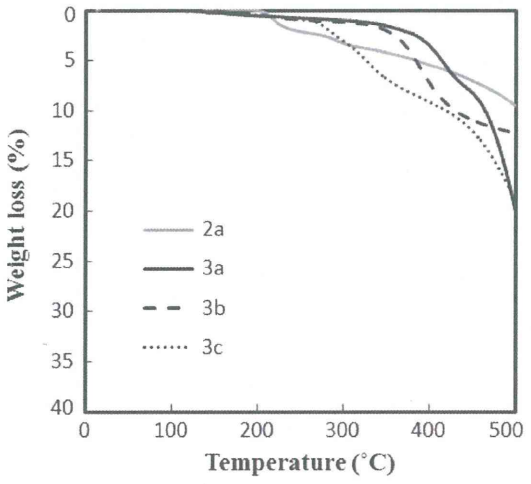


**Figure 2.** TGA chart of noncyclic acetal **2a** and cyclic **3a–c** under nitrogen flow with heating rate at 10 °C/min.

contrast, the first weight loss of **2a** up to 300 °C is 3.9 wt % which corresponds to the wt % of one methoxy group. The weight loss of **3** up to 400–420 °C is 6–10 wt % which almost corresponds to the diol moiety.

The degradation temperature of cyclic acetals **3** is slightly higher than that of double Diels–Alder bisadduct of bis(isobenzofuran)s (300 °C)[14] and far more higher than the monoadduct of isobenzofuran (220 °C).[15] The effect of ring-strain in five- to seven-membered cyclic acetals **3** seems to be a very important factor on the thermal stability[16] and the five-membered **3a** was the most thermally stable derivative among these acetalized fullerenes. Indeed, the relative ring strain energy $\Delta SE_{rel}$ (vs five-membered **3a**) estimated by PM3 calculation using isodesmic reaction method[17] showed the considerable increase by 16.3 and 21.9 kJ/mol for six-membered **3b** and seven-membered **3c**, respectively (Fig. 3). Interestingly, the increased strain energy was well reflected on the increasing acetal bond angle ∠O–C–O (cf. **2b**: 95.7°) and dihedral angle ∠O–C–C–H at spiro-ring, probably because of suffering from the eclipsed conformation with the adjacent methylene group in twist-boat conformation of cyclohexane ring.[20]

The less strain energy of five-membered spiro-acetal ring is somewhat unusual because, in the simple cycloalkane chemistry, the ring strain of six-membered ring is slightly smaller than that of five-membered ring.[21] To elucidate this discrepancy, we also conducted the strain energy calculations for the comparable five- to seven-membered ring skeletons, such as acetalized fullerenes **3**, spiro-acetals **4**, cyclic acetals **5**, and cycloalkanes **6** (Fig. 4). As expected, the strain energy of six-membered ring for cyclic acetal **5b** and cycloalkane **6b** was the lowest among the three ring sizes, respectively. However, the acetalized fullerene **3a** and spiro-acetal **4a** provided the lowest strain energy in the relevant five-membered ring. These results imply that the structure of *spiro*-linkage of acetal ring is responsible for the higher stability (less strain) of five-memberd **3a**.

It is also noteworthy that the spiro-linked cyclohexane ring in **3a** adopts the boat-form, in contrast to the favorable chair-form of **4a**, due to the rigidity of fullerene cage. Despite the difference in cyclohexane ring conformation between **3** and **4**, the five-membered ring is less strained than the six-membered ring in the present *spiro*-acetal ring structure. In addition to the thermodynamic stability, the kinetic factor (i.e., $\Delta G^{\ddagger}$) on the thermal degradation reaction should also be discussed. As discussed above, the strain energy of *spiro*-linked acetal fullerenes **3a–c** would play a crucial role in their thermal stability, mainly depressing the $\Delta H^{\ddagger}$ term. In addition, a possible reverse ring-closure of the ring-opened intermediate would be more facilitated in the order of five >six >seven-memebered ring due to the favorable $\Delta S^{\ddagger}$ in conformity with the present thermal stability of **3a–c**.[21]

The hydrolysis of acetal fullerene **3b** was also examined (Scheme 2). The addition of a catalytic amount of *p*-tosyl acid (50 mol %) into the toluene solution of **3b** at room temperature resulted in the deprotection reaction to reproduce **1** almost quantitatively after 12 h. The solubility of **3b** is enough high in many common solvents such as toluene, chloroform, and THF, while **1** is less soluble even in toluene. The appreciable solubility change in going from **3** to **1** under the mild acid-treatment seems to be an attractive property for utilization in EUV photoresist materials[18] or in wet process on fabrication of solar cells to stack thin layers without degradation of the underlying layer.[19] The hydrolysis rate of cyclic benzophenone acetals has been reported in the order of seven >six >five-membered rings, consistent with the order of ring strain as calculated.[22]

A plausible mechanism for the present acetalization is illustrated in Scheme 3. Initially, the coordination of $TiCl_4$ or its alkoxide analogue $TiL_4$ (L = Cl or OR)[10] on C=O group induces a

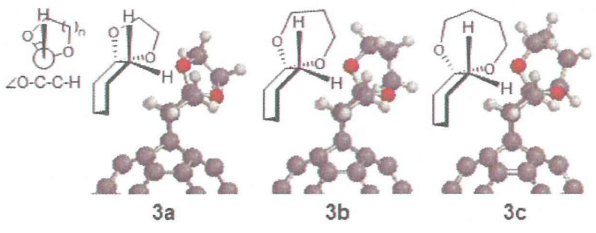


| calc. | 3a | 3b | 3c |
|---|---|---|---|
| $\Delta SE_{rel}$ (kJ/mol)[a] | 0 | +16.3 | +21.9 |
| ∠O–C–O (°) | 105.3 | 111.0 | 111.7 |
| ∠O–C–C–H (°) | 15.37 | 21.91 | 23.53 |

[a] Relative strain energy: *SE* relative to **3a**, where *SE* (**3a**) = $\{\Delta H_f(\mathbf{3a}{:}C_{66}H_{10}O_2) + 2\Delta H_f(CH_4)\} - \{\Delta H_f(\mathbf{2a}{:}C_{66}H_{12}O_2) + \Delta H_f(C_2H_6)\}$.

**Figure 3.** Optimized structure, relative strain energy $\Delta SE_{rel}$, acetal bond angle ∠O–C–O and dihedral angle ∠O–C–C–H of **3a–c** calculated at PM3 level.

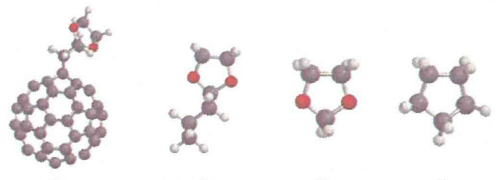


| ring size | 5 (**a**)[a] | 6 (**b**) | 7 (**c**) |
|---|---|---|---|
| acetalized fullerene **3** | 0 | +16.3 | +21.9 |
| spiro-acetal **4** | 0 | +17.3 | +24.1 |
| cyclic acetal **5** | 0 | –3.8 | +1.9 |
| cycloalkane **6** | 0 | –7.2 | +16.2 |

[a] Relative strain energy $\Delta SE_{rel}$ (kJ/mol): *SE* relative to 5-membered ring.

**Figure 4.** Comparison of strain energy $\Delta SE_{rel}$ on ring size (five, six, and seven-membered ring) for compounds **3–6** calculated at PM3 level.

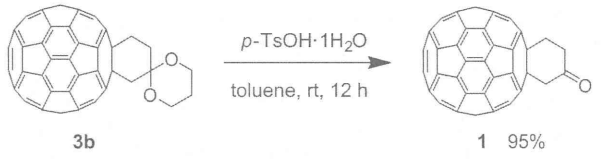


**Scheme 2.** Acid-catalyzed hydrolysis of acetal fullerene **3b**.

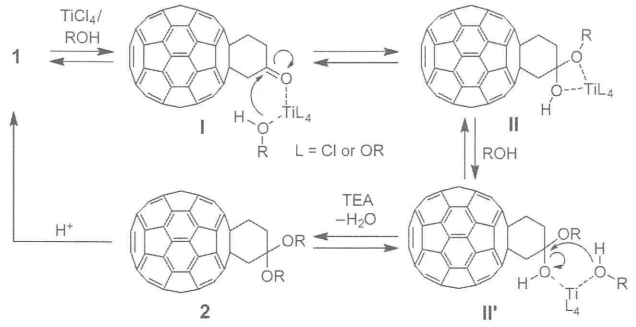


**Scheme 3.** Plausible reaction mechanism for Ti-mediated acetalization of fullerenyl ketone **1**.

nucleophilic attack of alcohol to the carbonyl carbon in **I**. Then, the formed hemiacetal intermediate **II**/**II**′ is again activated by Ti-catalyst to undergo the second substitution to give the acetal **2**. Because these steps may be reversible, the reaction requires an excess alcohol and dry solvent. The addition of triethylamine (TEA) in the final step quenches the Ti-catalyst to give **2**. The intermediate hemiacetal **II** was not detected in the crude reaction mixture due to the more labile property as compared with the corresponding acetal **2**.

In conclusion, novel acetalized fullerene derivatives were facilely synthesized from cyclohexanone-fused precursor in good yields. The various primary aliphatic alcohols and diols can be employed while the secondary alcohol did not react. The acetal fullerenes showed slightly raised LUMO energy level up to 0.04 eV than that of PCBM. The acetal moiety can be easily removed by acid catalyst and change the solvent solubility. Moreover, the cyclic acetal derivatives having a unique spiro-ring showed high thermal stability up to 350 °C under nitrogen atmosphere, depending on the ring strain. The further investigation on organic thin-film solar cell application as well as on EUV resist materials application of acetalized fullerenes is now undertaken and will be reported in detail elsewhere.

## Acknowledgments

This work was partially supported by JSPS KAKENHI of a Grant-in-Aid for Challenging Exploratory Research No. 23651111 and by Health Labor Sciences Research Grants from the Ministry of Health, Labor, and Welfare of Japan (MHLW).

## Supplementary data

Supplementary data (synthetic procedures, $^{1}H$ and $^{13}C$ NMR spectra and HRMS data for new compounds **2a–c** and **3a–c**) associated with this article can be found, in the online version, at http://dx.doi.org/10.1016/j.tetlet.2013.04.093.

## References and notes

1. (a) Peet, J.; Heeger, A. J.; Bazan, G. C. *Acc. Chem. Res.* **2009**, *42*, 1700; (b) Matsuo, Y. *Chem. Lett.* **2012**, *41*, 754.
2. (a) Kim, J. Y.; Lee, K.; Coates, N. E.; Moses, D.; Nguyen, T.-Q.; Dante, M.; Heeger, A. J. *Science* **2007**, *317*, 222; (b) Matsumoto, F.; Moriwaki, K.; Takao, Y.; Ohno, T. *Synth. Metals* **2010**, *160*, 961; (c) Li, C.-Z.; Chien, S.-C.; Yip, H.-L.; Chueh, C.-C.; Chen, F.-C.; Matsuo, Y.; Nakamura, E.; Jen, A. K.-Y. *Chem. Commun.* **2011**, *47*, 10082; (d) Matsuo, Y.; Okada, H.; Maruyama, M.; Sato, H.; Tobita, H.; Ono, Y.; Omote, K.; Kawachi, K.; Kasama, Y. *Org. Lett.* **2012**, *14*, 3784.
3. (a) Matsuo, Y.; Sato, Y.; Niinomi, T.; Soga, I.; Tanaka, H.; Nakamura, E. *J. Am. Chem. Soc.* **2009**, *131*, 16048; (b) He, Y.; Chen, H.-Y.; Hou, J.; Li, Y. *J. Am. Chem. Soc.* **2010**, *132*, 1377.
4. (a) An, Y.-Z.; Anderson, J. L.; Rubin, Y. *J. Org. Chem.* **1993**, *58*, 4799; (b) Ohno, M.; Azuma, T.; Kojima, S.; Shirakawa, Y.; Eguchi, S. *Tetrahedron* **1996**, *52*, 4983.
5. (a) An, Y.-Z.; Chen, C.-H. B.; Anderson, J. L.; Sigman, D. S.; Foote, C. S.; Rubin, Y. *Tetrahedron* **1996**, *52*, 5179; (b) Chamberlain, T. W.; Camenisch, A.; Champness, N. R.; Briggs, G. A. D.; Benjamin, S. C.; Ardavan, A.; Khlobystov, A. N. *J. Am. Chem. Soc.* **2007**, *129*, 8609.
6. Yang, J.; Alemany, L. B.; Driver, J.; Hartgerink, J. D.; Barron, A. R. *Chem. Eur. J.* **2007**, *13*, 2530.
7. See recent review: Li, C.-Z.; Yip, H.-L.; Jen, A. K.-Y. *J. Mater. Chem.* **2012**, *22*, 4161.
8. See recent review: Sanders, D. P. *Chem. Rev.* **2010**, *110*, 321.
9. (a) Torres-Garcia, G.; Mattay, J. *Tetrahedron* **1996**, *52*, 5421; (b) Yen, C.-F.; Peddinti, R. K.; Liao, C.-C. *Org. Lett.* **2000**, *2*, 2909.
10. Clerici, A.; Pastori, N.; Porta, O. *Tetrahedron* **2001**, *57*, 217.
11. *Compound data for* ***2a***: $^{1}H$ NMR (270 MHz, $CS_2/CDCl_3$) $\delta$ 3.02–3.07 (m, 2H), 3.48–3.52 (m, 2H), 3.53 (s, 6H), 3.74 (s, 2H); $^{13}C$ NMR (150 MHz) $\delta$ 33.63, 36.08, 45.05, 48.13 (2C), 61.71, 64.15, 101.96, 130.40, 135.10, 135.60, 140.07, 141.48, 141.51, 141.95, 141.99, 142.00, 142.47, 143.15, 144.61, 144.66, 145.11, 145.23, 145.32, 145.33, 145.36, 145.48, 146.13, 146.29, 146.35, 146.79, 146.91, 147.56, 147.59, 156.20, 157.27; MALDI-TOF MS, calcd for $C_{66}H_{12}O_2$ [$M^-$], 836.0832, found 836.0839. *Compound data for* ***3a***: $^{1}H$ NMR ($CDCl_3$) $\delta$ 3.15–3.20 (m, 2H), 3.51–3.56 (m, 2H), 3.72 (s, 2H), 4.19–4.32 (m, 4H); $^{13}C$ NMR $\delta$ 36.12, 36.31, 46.10, 61.86, 63.79, 64.71 (2C), 109.74, 135.35, 135.73, 140.19, 140.23, 141.62, 141.65, 142.10, 142.11, 142.12, 142.20, 142.59, 142.60, 143.28, 144.76, 144.80, 145.24, 145.34, 145.45, 145.48, 145.51, 145.64, 145.97, 146.27, 146.29, 146.44, 146.49, 147.72, 147.76, 156.35, 157.37; MALDI-TOF MS, calcd for $C_{66}H_{10}O_2$ [$M^-$], 834.0686, found 834.0687.
12. Wong, W. Y.; Wang, X.-Z.; He, Z.; Djurii, A. B.; Yip, C.-T.; Cheung, K.-Y.; Wang, H.; Mak, C. S. K.; Chan, W. K. *Nat. Mater.* **2007**, *6*, 521.
13. (a) Kooistra, F. B.; Knol, J.; Kastenberg, F.; Popescu, L. M.; Verhees, W. J. H.; Kroon, J. M.; Hummelen, J. C. *Org. Lett.* **2007**, *9*, 551; (b) Murata, M.; Morinaka, Y.; Murata, Y.; Yoshikawa, O.; Sagawa, Y.; Yoshikawa, S. *Chem. Commun.* **2011**, *47*, 7335; (c) Liu, C.; Xiao, S.; Shu, X.; Li, Y.; Xu, L.; Liu, T.; Yu, Y.; Zhang, L.; Liu, H.; Li, Y. *ACS Appl. Mater. Interfaces* **2012**, *4*, 1065; (d) Li, Y. *Acc. Chem. Res.* **2012**, *45*, 723.
14. Sander, M.; Jarrosson, T.; Chuang, S.-C.; Khan, S. I.; Rubin, Y. *J. Org. Chem.* **2007**, *72*, 2724.
15. Chuang, S.-C.; Sander, M.; Jarrosson, T.; James, S.; Rozumov, E.; Khan, S. I.; Rubin, Y. *J. Org. Chem.* **2007**, *72*, 2716.
16. (a) Cope, A. C.; Ambros, D.; Ciganek, E.; Howell, C. F.; Jacura, Z. *J. Am. Chem. Soc.* **1959**, *81*, 3153; (b) Jakab, E.; Till, F.; Székely, T.; Kozhabekov, S. S.; Zhubanov, B. A. *J. Anal. Appl. Pyrol.* **1992**, *23*, 229.
17. Caramori, G. F.; Galembeck, S. E.; Laali, K. K. *J. Org. Chem.* **2005**, *70*, 3242.
18. Oizumi, H.; Tanaka, K.; Kawakami, K.; Itani, T. *Jpn. J. Appl. Phys.* **2010**, *49*, 06GF04.
19. O'Malley, K. M.; Li, C.-Z.; Yip, H.-L.; Jen, A. K.-Y. *Adv. Energy Mater.* **2012**, *2*, 82.
20. Other relevant dihedral angles showed the similar tendency **3a** < **3b** < **3c** to the one shown in the table of Figure 3; 17.04 < 17.57 < 18.83 for $\angle O_{ax}$–C–C–H (°) and 14.45 < 16.63 < 17.30 for $\angle CH_2$–C–C–$CH_2$.
21. Eliel, E. L.; Wilen, S. H.; Mander, L. N. *Stereochemistry of Organic Compounds*; Wiley-Interscience: New York, 1994. pp 675–682, Chapter 11.3.
22. Oshima, T.; Ueno, S.; Nagai, T. *Heterocycles* **1995**, *40*, 607.

J Nanopart Res (2013) 15:1755
DOI 10.1007/s11051-013-1755-6

RESEARCH PAPER

# Magic number effect on cluster formation of polyhydroxylated fullerenes in water–alcohol binary solution

**Yuji Nakamura · Hiroshi Ueno · Ken Kokubo · Naohiko Ikuma · Takumi Oshima**

Received: 27 February 2013 / Accepted: 27 May 2013


**Abstract** Due to the spherical shape with a diameter of ca. 1 nm, the aggregation behaviour of fullerene $C_{60}$ is very interesting in view of the possible formation of magic number particle in a similar manner as metal cluster in gas phase. Herein, we report for the first time the magic number aggregation behaviours of polyhydroxylated fullerenol $C_{60}(OH)_{36}$ in water–alcohol (methanol, ethanol and 1-propanol) binary solution with increasing alcohol component. The diameters of particle were ca. 6–8 nm depending on the alcohol used. The particle sizes were precisely measured by the novel-induced grating method which is superior for the particle-size measurement in single-nano region (1–10 nm). The magic number cluster was also detected by scanning probe microscopy observation. However, such aggregation behaviours were not found in DMSO–alcohol system or for the use of less hydroxylated $C_{60}(OH)_{10}$.

**Keywords** Magic number cluster · Polyhydroxylated fullerenes · Induced grating (IG) method · Nanoparticle

Y. Nakamura · H. Ueno · K. Kokubo (✉) · N. Ikuma · T. Oshima
Division of Applied Chemistry, Graduate School of Engineering, Osaka University, 2-1 Yamadaoka, Suita, Osaka 565-0871, Japan
e-mail: kokubo@chem.eng.osaka-u.ac.jp

## Introduction

The magic number effect in metal cluster formation has been of great theoretical interest (Anagnostatos 1987; Sattler 1993; Garvey et al. 1994). It has been proposed that the magic numbers, mostly found in mass spectra, originate from (i) the closed electronic shell structure comprising delocalized valence electrons in alkali- and noble-metal clusters ($n = 8, 20, 40,\ldots$) and (ii) geometrically stable structures, such as an icosahedron, in the rare-gas atom clusters for main shell numbers ($n = 13, 55, 147,\ldots$) and for the subshell numbers ($n = 19, 23, 25,\ldots$) (Sakurai et al. 1999). Interestingly, the magic number effect has also been reported for nonmetal fullerene clusters of $(C_{60})_n$ ($n = 13, 19, 27, 39, 55$, etc.) (Martin et al. 1993; Branz et al. 2002), especially for icosahedral symmetry of $n = 13$ and 55 (Hansen et al. 1996). Such effect has been recognized only under mass spectrometric measurement, in spite of a fact that $C_{60}$ has been known to form aggregates in various solvents (Ying et al. 1994; Nath et al. 1998; Kyzyma et al. 2010; Brant et al. 2005; Deguchi et al. 2006). It is likely that the aggregation of $C_{60}$ is due to some intermolecular weak interaction such as van der Waals force and π–π interaction which may compete with the analogous interaction with solvents. Thus, the cluster formation of $C_{60}$ in solution needs the chemical modification of the spherical fullerene surface which can intensify the self-aggregation and compete or overcome the solute–solvent interactions.

Published online: 07 June 2013

An effective strategy for enhancing the intermolecular interaction between $C_{60}$ molecules involves the introduction of many hydroxyl groups, which also makes them soluble in polar solvents. Recently, we have synthesized highly polyhydroxylated fullerenes, fullerenols $C_{60}(OH)_{36}\cdot 8H_2O$ and $C_{60}(OH)_{44}\cdot 8H_2O$, and found that the particle size of these fullerenols is ca. 1 nm in water and DMSO, which is consistent with their monodispersity based on the molecular size (Fig. 1) (Kokubo et al. 2008; Kokubo et al. 2011). The solution behaviour of these fullerenols is governed primarily by hydrogen bonds as well as dipole–dipole interactions between the fullerenol molecules, fullerenol–solvent molecules and solvent molecules.

In this context, it is very interesting to know the aggregation behaviour of functionalized fullerenol when the interaction with the surrounding solvent is gradually turned by using less polar binary solvent system. To our own surprise, the magic number effect was observed for the first time for fullerene solution chemistry and we reported the detailed aggregation behaviour of fullerenols in various water–alcohol binary solutions. We rely on the newly developed induced grating (IG) measurement to precisely assess the particle sizes in solution (Wada et al. 2006). The IG method based on the light diffraction takes advantage of reproducibility of size measurement due to the less affection of impurities, especially in the single-nano region (1–10 nm) as compared with the conventional dynamic light scattering (DLS) technique.

## Experimental

### Materials and instruments

$C_{60}(OH)_{10}$ was purchased from Frontier Carbon Corporation (as nanom spectra D100). $C_{60}(OH)_{36}\cdot 8H_2O$ was prepared by the previously reported method (Kokubo et al. 2008). All other reagents were commercially available and used without further purification. Particle-size measurement was performed using a Shimadzu IG-1000 and Shimadzu SPM-9700. Zeta-potential measurement was conducted using a Malvern Zetasizer nano ZS.

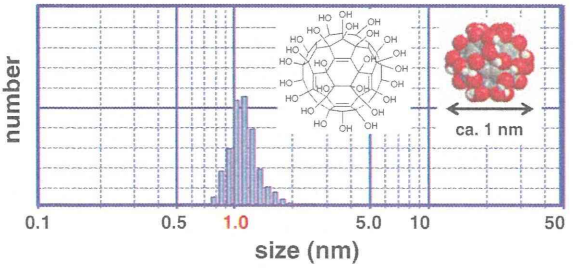


**Fig. 1** Possible structure and particle-size distribution measured by IG method of $C_{60}(OH)_{36}$ in DMSO (1 mM)

### Induced grating method particle-size measurement

A water (or DMSO) solution of fullerenol (10 mM) was diluted with water (or DMSO) to a certain concentration and was sonicated for 10 s. Then, the corresponding molar amount of second solvent (alcohols or acetonitrile) was added and sonicated again for 10 s to obtain the sample solution (1 mM) for particle-size measurement. A cuvette containing the sample solution (ca. 250 μL) was introduced into IG-1000 and an electrode was inserted to the cuvette. The cuvette was calmly left for several minutes at 25 °C before the measurement. Viscosity of the solvent was inputted as a parameter and the electrophoresis condition was appropriately optimized by changing voltage, frequency and application time. The values of viscosity for mixed solvents were obtained from the references (Bhuiyan et al. 2007; Grande et al. 2009; González et al. 2007; Mikhail and Kimel 1963). After the measurement, the particle-size distribution by number was calculated using the data ranging from 1/2 to 3/4 of photo-intensity obtained. Each measurement was conducted ten times for the same sample solution.

### SPM particle-size measurement

A ethanol/water binary solution (0.1 μM for 0/100 and 0.1 mM for both 30/70 and 80/20) of $C_{60}(OH)_{36}\cdot 8H_2O$ was applied to a mica plate (5 μL) and dried it at room temperature before the measurement.

### Zeta-potential measurement

The zeta-potential values were determined as the average of four times measurements. The value of dielectric constant of ethanol was substituted for that of mixed solvent.

## Results and discussion

Measurement of the particle size by IG was performed using two fullerenols, i.e., less-hydroxylated water-

insoluble $C_{60}(OH)_{10}$ and water-soluble $C_{60}(OH)_{36}$. Both fullerenols exhibit high solubility in DMSO (1 mM), resulting in a narrow particle-size distribution at ca. 1 nm, consistent with the molecular size (Fig. 1). Incidentally, the similar small particle size was also confirmed by DLS for $C_{60}(OH)_{36}$ in water (Kokubo et al. 2011), although this method provided the aggregation size at around 100 nm for less polar $C_{60}(OH)_{18}$ (Mohan et al. 1998) and $C_{60}(OH)_{24}$ (Chae et al. 2009) by DLS in water. First, the particle sizes of $C_{60}(OH)_{10}$ were measured in a binary solution which was made by adding varying mol% of co-solvent MeOH, EtOH, or MeCN into the DMSO solution of fullerenol (Fig. 2). Each point was measured at least 10 times, and the standard deviations are indicated by error bars. Addition of alcohols to over 60 mol% brought about appreciable aggregation with particle sizes up to 30–50 nm. More than 80 mol% addition induced the formation of a suspension (>200 nm) along with the formation of small aggregates. Comparable monotonous size increase as percolation cluster (Semenov et al. 2011) was observed for highly hydroxylated $C_{60}(OH)_{36}$ in the same binary solvent (Fig. 3).

However, the remarkably different aggregation behaviours of the $C_{60}(OH)_{36}$ species were observed in *water*-based binary solvent (Fig. 4). Noticeably, the increasing addition of alcohol brought about the primary abrupt raising curve up to the metastable particle size of 6–8 nm and the further addition of alcohol resulted in the expected aggregation behaviour. The inflection point drastically moves from

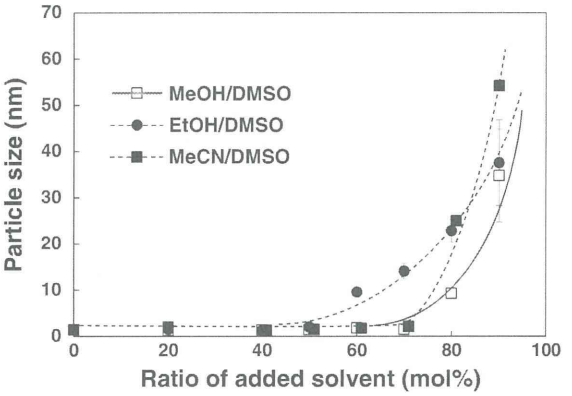


**Fig. 3** Aggregate particle size of $C_{60}(OH)_{36}$ in the mixed solvents (1 mM) of DMSO with MeOH (*open square*), EtOH (*filled circle*) and MeCN (*filled square*)

50 mol% MeOH, through 30 mol% EtOH, to 17 mol% 1-PrOH, respectively. We believe that this intriguing aggregation behaviour can be ascribed to the magic number effects on cluster formation of $C_{60}(OH)_{36}$ in water–alcohol binary system. As similar stepwise growth of metastable fullerene clusters in solution has never been reported, this is the first report of magic number effects on the aggregation behaviour of $C_{60}(OH)_{36}$.

The aggregation behaviour of nanoparticles is well explained by the conventional DLVO theory (Young et al. 1993). Thus, it is natural that the aggregation occurs in the case of the less polar 1-PrOH at a lower mol% as compared with EtOH and MeOH, because the longer alkyl group $R$ = 1-Pr can reduce the solvent (water) polarity to a greater extent than the other

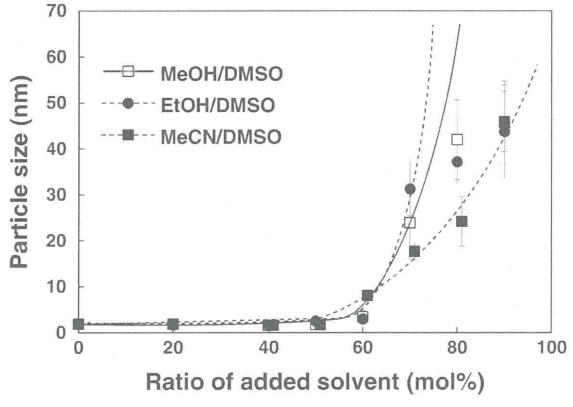


**Fig. 2** Aggregate particle size of $C_{60}(OH)_{10}$ in the mixed solvents (1 mM) of DMSO with MeOH (*open square*), EtOH (*filled circle*) and MeCN (*filled square*)

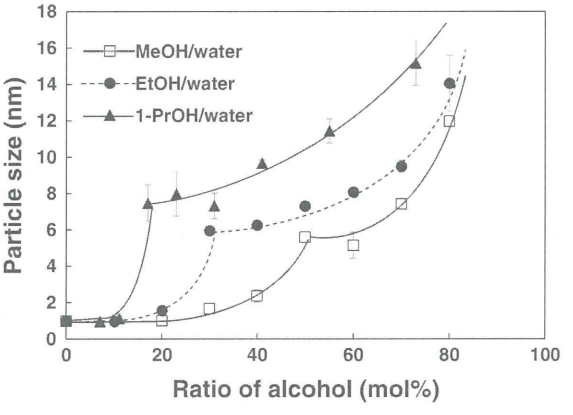


**Fig. 4** Aggregate particle size of $C_{60}(OH)_{36}$ in the mixed solvents (1 mM) of water with MeOH (*open square*), EtOH (*filled circle*) and 1-PrOH (*filled triangle*)

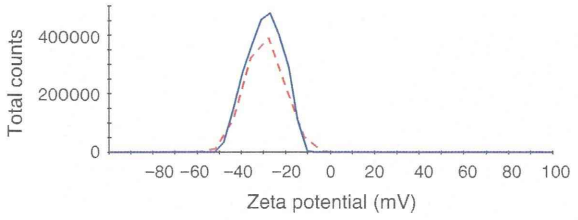


**Fig. 5** Zeta potential of $C_{60}(OH)_{36}$ in water (*solid*) and water–EtOH (80 mol% of EtOH; *dashed*)

alcohols. The reduction of the solvent polarity may enhance the electrostatic interaction between fullerenol molecules, thereby forming the cluster. Thus, we measured the zeta-potential ($\zeta$) of $C_{60}(OH)_{36}$ using DLS particle-size analysis (Fig. 5). However, $\zeta$ in water (−29.3 mV) was not drastically different from the value (−29.5 mV) in water–EtOH (80 mol% of EtOH), although clusters of ca. 14 nm were observed in this binary solvent (Fig. 4). Therefore, the behaviour

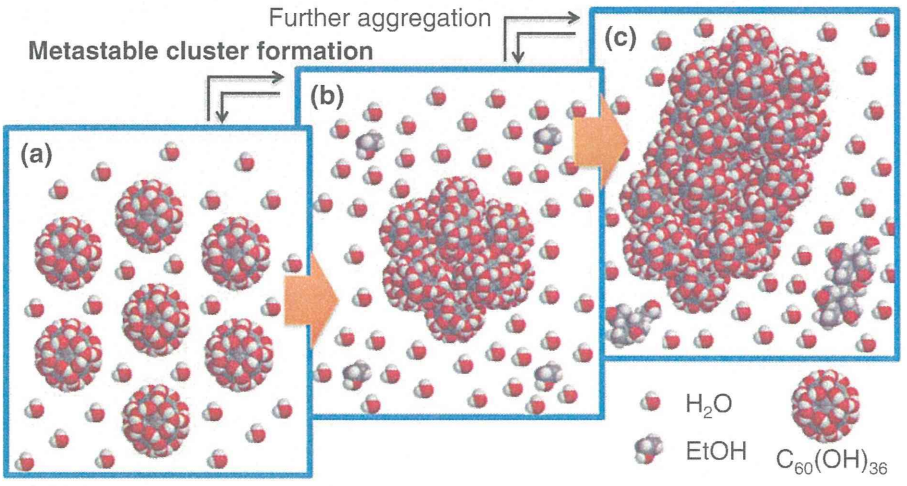


**Fig. 6** Illustrative formation mechanism of metastable clusters of $C_{60}(OH)_{36}$ in water–alcohol binary solvent

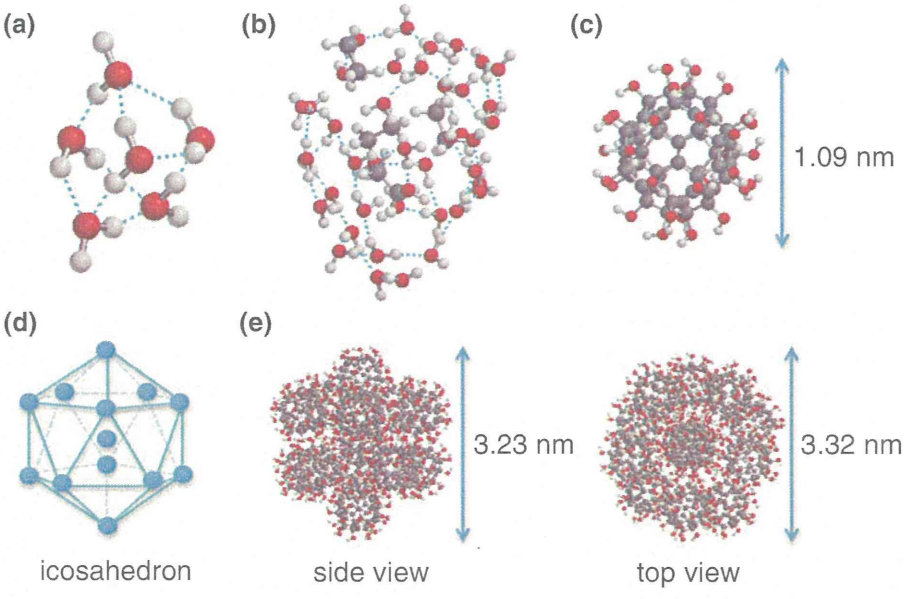


**Fig. 7** Molecular mechanics simulation of **a** $H_2O$, **b** $4EtOH + 36H_2O$, **c** a possible isomer of $C_{60}(OH)_{36}$, **d** structure of icosahedron and **e** icosahedral 13-mer of $C_{60}(OH)_{36}$

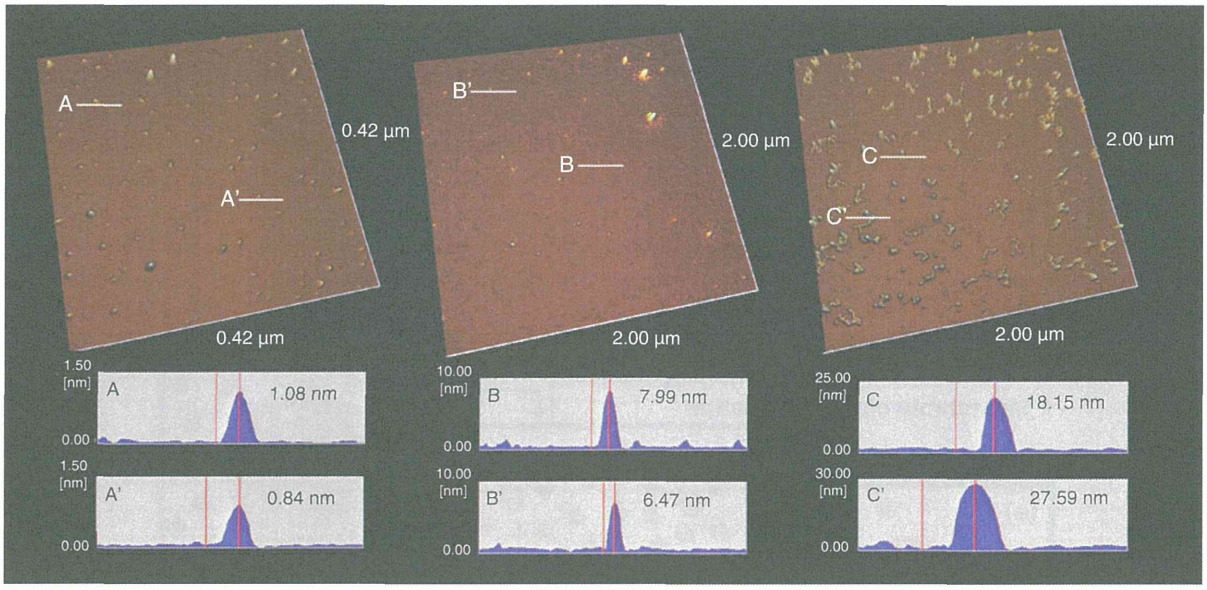


**Fig. 8** SPM single-particle analysis of metastable clusters of $C_{60}(OH)_{36}$ in water–alcohol binary solvent. The diluted solutions were applied to a mica plate and dried it before observation. *A* In EtOH/water = 0/100, *B* 30/70 and *C* 80/20

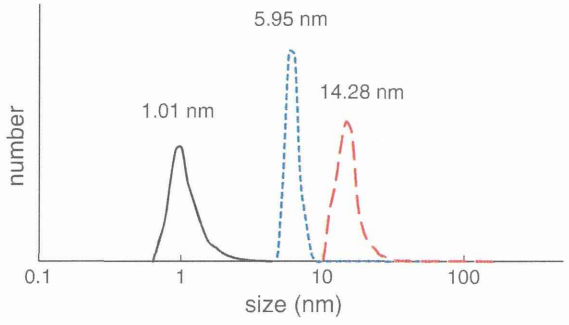


**Fig. 9** Particle-size distribution of $C_{60}(OH)_{36}$ measured by IG method in the mixed-solvent of water with ethanol (*solid*: 0, *dotted*: 30, *dashed*: 80 mol%)

of the present fullerenol may be governed by the solute–solvent interaction. Specifically, the alcohol *R*-groups can essentially achieve hydrophobic interaction with the surrounding water to reduce the effective amount of bulk water and thereby somewhat inhibit the hydrogen bond stabilization of $C_{60}(OH)_{36}$. This unfavourable effect should increase in the following order: 1-PrOH > EtOH > MeOH; thus, the aggregation of $C_{60}(OH)_{36}$ would be accelerated in this order, which adequately accounts for the left side shift of the magic number composition (mol%) of the alcohols.

Based on the above results, a plausible mechanism for the formation of the metastable $C_{60}(OH)_{36}$ magic number cluster is illustrated in Fig. 6. Fullerenol molecules are highly solvated in water by strong hydrogen bonds (Figs. 6a, 7a) (Rodríguez-Zavala et al. 2011). Addition of alcohol molecules seems to weaken the hydrogen bond network of water molecules comprising the inherent water cluster structure around the alcohol *R* group. As previously reported (Wakisaka et al. 2001), the layer structure composed of nearly equal numbers of alcohol and water molecules is formed from stable binary clusters (Figs. 6b, 7b). Further addition of alcohol molecules leads to the formation of the self-aggregating alcohol clusters. During this self-aggregating step which requires more than 35 mol% for methanol, 15 mol% for ethanol and 5 mol% for 1-PrOH, the aggregate size of the fullerenol cluster remains unchanged. In other words, the appreciable hydrophobic *alcohol–water* interaction overcomes the *fullerenol–water* interaction in the combined water–alcohol binary phase. Finally, addition of much larger amount of alcohol results in larger secondary aggregates (Fig. 6c). The fullerenol cluster size was estimated by performing molecular mechanics calculation. The diameter of icosahedral 13-mer of $C_{60}(OH)_{36}$ was calculated and found to be ca. 3.3 nm (Fig. 7e). Therefore, the present metastable cluster with a diameter of 6–8 nm can be estimated to be as large as 55-mer (Boyen et al. 2002) (ca. 5.55 nm, if the incorporated water is ignored).